Interatomic potential for uranium in a wide range of pressures and temperatures

2012 J. Phys.: Condens. Matter 24 015702

(http://iopscience.iop.org/0953-8984/24/1/015702)

IOP PUBLISHING JOURNAL OF PHYSICS: CONDENSED MATTER
J. Phys.: Condens. Matter **24** (2012) 015702 (8pp) doi:10.1088/0953-8984/24/1/015702

Interatomic potential for uranium in a wide range of pressures and temperatures

D E Smirnova[1], S V Starikov[1,2] and V V Stegailov[1,2,3]

[1] Joint Institute for High Temperatures, Russian Academy of Sciences, Moscow 125412, Russia
[2] Moscow Institute of Physics and Technology, Dolgoprudny 141700, Russia
[3] All-Russia Research Institute of Automatics (VNIIA), Moscow 127055, Russia

E-mail: d.e.smirnov@gmail.com

Received 12 September 2011, in final form 14 November 2011
Published 2 December 2011
Online at stacks.iop.org/JPhysCM/24/015702

Abstract
Using the force-matching method we develop an interatomic potential that allows us to study the structure and properties of α-U, γ-U and liquid uranium. The potential is fitted to the forces, energies and stresses obtained from *ab initio* calculations. The model gives a good comparison with the experimental and *ab initio* data for the lattice constants of α-U and γ-U, the elastic constants, the room-temperature isotherm, the normal density isochore, the bond-angle distribution functions and the vacancy formation energies. The calculated melting line of uranium at pressures up to 80 GPa and the temperature of the α–γ transition at 3 GPa agree well with the experimental phase diagram of uranium.

(Some figures may appear in colour only in the online journal)

1. Introduction

Uranium is a key component of nuclear fuels. For several decades metallic fuels have been overshadowed by oxide and ceramic fuels. However, nowadays uranium alloys are under active investigation as possible fuels for future fast and research reactors [1–4]. Understanding of the radiation damage effects on the fuel stability is one of the major challenges to be solved on the way to effective and safe fuel design. The description of the radiation damage requires a knowledge of the atomistic mechanisms of defect generation in solids [5, 6]. However, they are still not sufficiently studied for metallic uranium compounds and atomistic models are not mature enough even for pure U.

Uranium has four possible structures: the orthorhombic α-U, the tetragonal β-U, the high-temperature bcc γ-U and liquid. The crystal structure of the low-temperature α-U is presented in figure 1. At temperature $T \sim 935$ K and zero pressure α-U transforms to β-U, which is stable in a very small range of pressures and temperatures. At 1045 K β-U transforms to γ-U, then at 1406 K γ-U melts. Solid α-U and γ-U allotropes and liquid uranium are of the most interest because these structures are directly involved in the technological processes of nuclear fuel operation.

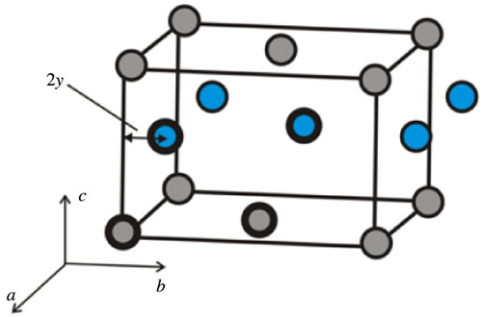

Figure 1. The crystal structure of α-U. Four basis atoms are marked.

The problem of investigation of the structure and elastic properties of solid uranium has been previously treated using density functional theory (DFT) based *ab initio* calculations. Söderlind [7] has performed *ab initio* calculations of the α-U equilibrium volume and bulk modulus within the all electron full-potential method. Later Taylor [8] applied the pseudo-potential developed for uranium by Kresse and Joubert [9] to calculate structure and elastic moduli of both α-U and γ-U. In addition, Taylor has obtained the value of a single vacancy formation energy for the low-temperature

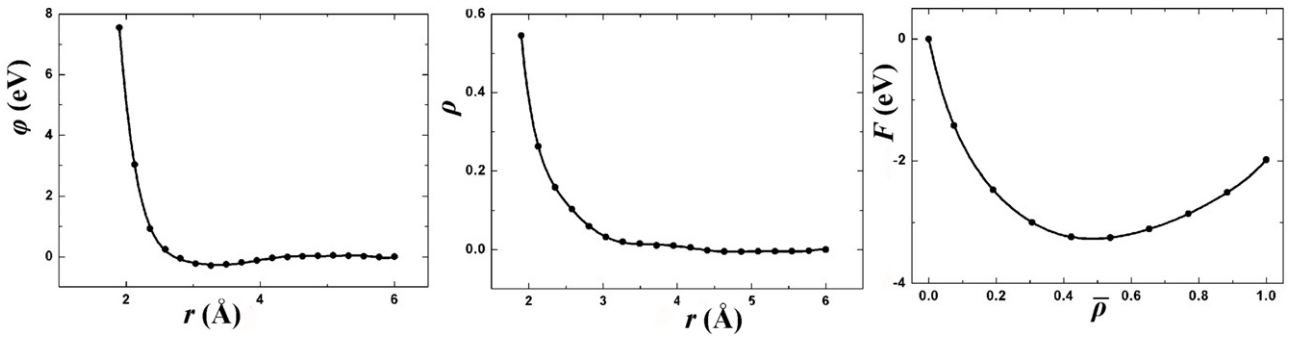

Figure 2. The EAM potential developed in this work. The potential is determined by three functions (see equation (1)): φ is the pair potential, ρ has a qualitative meaning of an effective electron density that is induced at the given atom by its neighbour atom, F is the embedding function that introduces many-body effects. The dots represent spline knots.

α-U. Xiang *et al* [10] have used the same pseudo-potential to calculate the properties of defects in the U–Nb system (including a single vacancy in pure uranium). Quantum molecular dynamics (QMD) simulations of solid and liquid U in a 54-atom model have been carried out in [11]. The results of a very detailed study of the possible defect formation in the solid uranium allotropes have been presented by Beeler *et al* [12]; they provided data on the energies of a single vacancy formation in α-U and γ-U allotropes, as well as the formation energies of self-interstitials, Zr interstitials and Zr substitutional defects for the bcc γ-U. First-principles study of the defect behaviour and diffusion mechanisms in α-U and α-U–Zr have been carried out in [13]. Landa *et al* have performed an *ab initio* study of γ-U–Mo and γ-U–Zr [14].

One can see that *ab initio* methods have been successfully applied to study various properties of solid uranium. However, the application of these DFT based *ab initio* techniques is limited by the maximum computationally possible model size ($\sim 10^2$ atoms) and time length (of the order of picoseconds). Such limitations essentially narrow the applicability of *ab initio* models for atomistic studies of phase transitions, plastic deformations, radiation damage etc. It is the classical molecular dynamics (MD) models that are able to move atomistic description forward to several orders of magnitude larger time and length scales. However, the accuracy of classical MD models is based on the accuracy of the interatomic potentials deployed. In this respect one can mention that the radiation damage studies of reactor materials show relatively more progress in comparison with fuels. The reason for this is the availability of the accurate interatomic potentials for iron and other relevant metals (e.g. [15–26]). The main general requirement to the interatomic potential is that it should capture all necessary features of the processes under consideration. For example, a correct description of the defect energies' hierarchy is very important for radiation damage models. If such a potential is at hand, then using current computational recourses it is possible not only to access via direct MD nanosecond and sub-micrometre time and length scales, but to create multiscale models that bridge the gap between atomistic and kinetic scales (e.g. see [27] and [28, 29]).

To our knowledge, there exist three published interatomic potentials for uranium [30–33]. All of them are developed as central-force many-body potentials [34–38] commonly referred to as embedded atom method (EAM) potentials [34, 35]. This type of many-body potential is widely used for simulating the interatomic interactions in metals. In this framework the potential energy of the system can be represented as follows:

$$U = \sum_{i<j} \varphi(r_{ij}) + \sum_j F(\bar{\rho}_j), \qquad \bar{\rho}_j = \sum_{j\neq i} \rho(r_{ij}). \quad (1)$$

This is an empirical model that has only qualitative physical justification based on first principles. The typical shapes of the functions in equations (1) are shown in figure 2. Qualitatively one can consider the first term as a sum of pair potentials φ over all atom pairs in the system (r_{ij} is the distance between atoms i and j). $\bar{\rho}$ is an effective electron density that is induced by the neighbouring atoms at the given atom (ρ gives a contribution from each neighbour). Both functions φ and ρ are short-ranged and in many EAM models go to zero at the same cut-off radius. A non-linear embedding function F introduces many-body effects. The curvature of F allows us to describe the lowering of the energy of a given atom when the number of its neighbours increases. This is impossible to do using only pair potentials but crucially important for modelling metallic bonding [34–38].

The construction of the above-mentioned potentials for U [30–33] was based on simple analytical forms of the φ, ρ and F functions. The potential of Pascuet *et al* [30, 31] was fitted to the lattice constants, the equilibrium atomic volume, the bulk modulus and the cohesion energy of α-U. The embedding function F was obtained from the universal features of the equation of state of metals. This potential describes α-U at normal conditions and qualitatively reproduces α-to-γ transition.

The potential developed by Belashchenko *et al* [32] was fitted to the data on the structure of liquid uranium in the vicinity of the melting temperature and to the results of high pressure impact tests. It gives an accurate description of the thermophysical properties of liquid uranium and bcc γ-U. The calculated density, self diffusion coefficient of the liquid phase and the melting line are all in good agreement with the experimental data. However this potential is not suitable for low-temperature α-U.

The potential of Li *et al* [33] was fitted to the *ab initio* results on the U_2 dimer energies, the fcc lattice constant and several other energetic and elastic properties of different structures. Liquid U properties were not considered. Only limited data on the accuracy of this potential were presented in [33].

Therefore none of the existing potentials describes simultaneously the properties of α-, γ-and liquid uranium and the corresponding transitions at the acceptable level of accuracy in a wide range of pressures and temperatures. Such a potential is the goal of this work.

2. Construction of the potential

The development of the *ab initio* DFT methods made it possible to include the *ab initio* data into the fitting database for potential parameter tuning. Initially *ab initio* data only supplemented the experimental data. In recent years, however, the interatomic potential fitting has tended to rely exclusively on the *ab initio* results. Probably the first completely *ab initio* based approach for potentials' development was originally proposed by Ercolessi and Adams [39] and called the force-matching method. In the recent work of Fellinger *et al* on Nb [40] a very detailed explanation of this method was given. Two authors of this work have recently constructed an EAM potential for Mo using the same technique [28]. In the force-matching method the whole developing process is divided into two stages. First the reference database is built. This reference database contains *ab initio* values of atomic forces, energies and stresses calculated for various atomic structures (so-called configurations). At the second stage the optimization of the EAM potential is performed. It is required to minimize the deviations between the reference *ab initio* values of forces, energies and stresses and their EAM approximations. The iterative minimization process results in a potential that reproduces the reference data with the best accuracy. We use the force-matching method as described below.

Table 1. The configurations database. The configurations represent various uranium structures under different conditions. N is the number of atoms in each configuration. The V/V_0 column lists the ratio of the given atomic volume V to the equilibrium experimental volume V_0 of α-U, γ-U [49, 54] and liquid U [32]. The T column lists the temperature value corresponding to the particular configuration. The Δ column lists the average fitting errors for the forces obtained with the resulting EAM potential (see equation (2)).

Configuration	Structure	N	V/V_0	T (K)	Δ (%)
1	α-U	120	1.000	900	0.41
2		120	1.000	770	0.41
3		120	1.004	850	0.40
4		120	1.060	990	0.38
5		120	1.000	1300	0.44
6		120	0.940	1200	0.37
7		120	0.902	1600	0.25
8		120	0.850	1600	0.24
9		120	0.827	1700	0.26
10		120	0.827	1100	0.34
11		120	0.902	550	0.35
12		120	1.000	372	0.27
13		120	0.941	340	0.24
14		120	1.061	390	0.27
15	γ-U	128	1.024	1140	0.46
16		128	0.988	1230	0.36
17		128	0.904	2100	0.28
18		128	0.772	3000	0.20
19		128	0.813	2300	0.21
20		128	0.787	2000	0.18
21		128	0.944	1550	0.29
22		128	0.847	1900	0.23
23		128	0.760	3100	0.20
24		128	0.825	1925	0.20
25	liquid U	54	1.293	4300	0.56
26		54	1.448	3077	1.30
27		128	0.934	4000	0.29
28		128	0.769	3740	0.16
29		128	0.934	5760	0.23
30		128	0.679	5140	0.15
31		128	0.748	4700	0.14
32		128	0.790	4000	0.20
33		128	0.734	5900	0.15
34		54	1.293	3417	1.10

2.1. The reference database

For computation of the reference database we need to create a set of reference structures. These structures represent α-U, γ-U and liquid uranium at different densities. Each reference structure contains about 120 atoms in a simulation box with the periodic boundary conditions in all three dimensions (3D PBC). For each of these structures we perform a short ($\sim$1 ps) MD-run with the trial potential [32] and at the given temperature T. This way we introduce thermal displacements of atoms the magnitudes of which reflect the given temperature. The final atomic arrangement after the MD calculation for a given initial structure is one of the required configurations. Classical MD calculations are performed using the LAMMPS code [41].

Then we perform *ab initio* DFT calculations of reference forces, per atom energies and stress tensors for each configuration using the plane-wave code VASP [42]. To represent the inner electronic structure of uranium we adopt a projector-augmented wave pseudo-potential developed by Kresse and Joubert [9] and previously used by Taylor [8]. The Perdew–Wang 91 exchange correlation functional [43] is also applied. We set the basis plane-wave energy cut-off equal to 500 eV. According to the symmetry of the structures studied we use the following k-point meshes: $3 \times 1 \times 2$ for α-U configurations and $2 \times 2 \times 2$ for γ-U and liquid U. These energy cut-offs and meshes provide converged DFT energies, forces and stresses.

The complete reference database contains 12 054 values of force components, 34 values of the per atom energy and 204 components of the stress tensor. The list of all configurations of the fitting database is given in table 1.

2.2. Fitting of the potential to the DFT reference data

The trial functions φ, ρ and F are chosen in the form of cubic splines. The spline knots are adjusted in an iterative way for minimizing the deviations between the reference

Table 2. The resulting knots of the cubic splines defining the EAM potential. For the pair potential φ and the electronic density function ρ 19 knots were adjusted. The embedding function $F(\bar{\rho}_j)$ is determined by ten knots (the last two columns).

n	r_{ij} (Å)	$\varphi(r_{ij})$ (eV)	$\rho(r_{ij})$	$\bar{\rho}_j$	$F(\bar{\rho}_j)$ (eV)
1	1.900 00	7.548 735 419 793 804 800	0.544 865 689 913 06	0.000 000	0.000 000 000 0000
2	2.127 77	3.027 262 284 620 461 300	0.262 383 777 458 72	0.075 017	−1.421 087 439 9504
3	2.355 55	0.932 256 757 441 457 200	0.158 804 074 772 49	0.190 640	−2.467 504 899 3797
4	2.583 33	0.241 865 209 658 825 880	0.103 490 323 489 83	0.306 263	−3.000 002 974 6112
5	2.811 11	−0.052 129 863 767 814 630	0.059 342 523 272 80	0.421 886	−3.240 883 065 4253
6	3.038 88	−0.234 471 524 509 781 090	0.031 902 062 136 11	0.537 509	−3.246 575 553 2375
7	3.266 66	−0.293 405 670 917 844 590	0.020 235 827 273 83	0.653 132	−3.112 401 064 7774
8	3.494 44	−0.252 497 357 178 855 960	0.015 146 623 921 70	0.768 754	−2.857 330 979 8021
9	3.722 22	−0.191 608 768 374 650 930	0.010 847 478 961 64	0.884 377	−2.505 042 439 2625
10	3.950 00	−0.120 662 870 486 473 710	0.010 511 579 029 66	1.000 000	−1.982 300 583 9202
11	4.177 77	−0.042 920 121 382 967 677	0.005 488 387 664 27		
12	4.405 55	−0.005 607 540 432 113 615	−0.002 039 192 143 85		
13	4.633 33	0.013 340 387 444 210 934	−0.004 896 963 138 58		
14	4.861 11	0.032 297 818 096 560 113	−0.005 337 327 018 87		
15	5.088 88	0.042 144 521 168 244 332	−0.004 276 624 061 33		
16	5.316 66	0.035 553 638 079 349 650	−0.004 595 188 524 57		
17	5.544 44	0.014 891 148 455 440 949	−0.004 051 151 490 15		
18	5.772 22	−0.004 642 055 500 075 333	−0.002 776 552 191 69		
19	6.000 00	0.000 000 000 000 000 000	0.000 000 000 000 00		

database values and the respective values calculated with the EAM potential. This operation is conducted by the code *potfit* [44, 45]. Then the resulting potential is verified by the test MD calculations of the structure and properties of uranium. Several test properties are compared with the known experimental data. If the agreement is not sufficient we modify the database structures (add or remove configurations, change their 'statistical weights' in the minimization scheme etc). Then we repeat the potential generation procedure once more. The optimized cubic splines representing the final potential functions φ, ρ and F are shown in figure 2. Table 2 presents the final values of the spline knots for all these functions [4]. We determine the average fitting errors for the forces in each reference configuration:

$$\Delta = \frac{1}{N}\sum_{i=1}^{N}\sqrt{\frac{\left(F^i_{\mathrm{EAM}} - F^i_{\mathrm{DFT}}\right)^2}{\left(F^i_{\mathrm{DFT}}\right)^2}}, \tag{2}$$

here N is the number of atoms in a given configuration, F_{EAM} is an EAM force, F_{DFT} is a reference DFT force.

From table 1 it can be seen that for all configurations consisting of 120–128 atoms the values of the errors are about 15–40% (depending on the uranium structure). For the high-temperature rarefied liquid configurations (with 54 atoms in a simulation box) fitting errors are more than 120%. The reason for such significant errors is that the cut-off radius of the potential (6 Å) is obviously insufficient for modelling highly expanded uranium.

3. Properties of solid uranium

To verify the potential we carry out MD calculations of the structural, mechanical and thermodynamic properties of the solid structures of uranium and address its phase diagram. Each of these models consists of 2000 atoms in 3D PBC. Additionally we examine the vacancy formation energies in α-U and γ-U.

3.1. Structure and elastic properties

We calculate the lattice parameters at zero pressure, the bulk modulus and other elastic constants of α-U and γ-U with the developed potential. The results are summarized in table 3. The elastic constants c_{ij} are calculated from MD simulations of uniaxial compression of solid α-U. The stress components change with deformation in a linear way (see figure 3). The elastic constants can be determined as follows (in Voigt notation):

$$c_{ij} = \frac{\Delta\sigma_{jj}}{\epsilon_{ii}}, \tag{3}$$

where $\Delta\ \sigma_{jj}$ is the change in the stress component along the j-axis providing that the model size l^0_i is slightly decreased and the corresponding deformation is:

$$\epsilon_{ii} = \frac{\Delta l_i}{l^0_i}. \tag{4}$$

The bulk modulus is determined from MD simulations of uniform compression and expansion with respect to the equilibrium volume:

$$B = -V_0\frac{\Delta P}{\Delta V}. \tag{5}$$

Here V_0 is the equilibrium volume of the solid (at $T \sim 300$ K for α-U and at the $T \sim 900\,^{\circ}$C for γ-U). The corresponding 'pressure–volume' dependence is a linear function of volume. The presented values of the bulk modulus are obtained in the range of $\Delta V/V_0 \sim 0.5$–6%. The elastic constants and the bulk modulus of α-U are within 10–30% of the experimental data. The errors are larger for c_{12} and c_{13}.

[4] The potential in the LAMMPS *setfl* format is available at www.ihed.ras.ru/norman/files/U.eam.sss.

Table 3. The EAM values of the lattice constants (a, b and c are presented in Å, y is given as a relative dimensionless value representing a fraction of b). The atomic volume (in Å^3), the bulk modulus (GPa), the elastic constants (GPa) and the cohesive energy (eV) of solid uranium structures are shown in comparison with the previous DFT based results and experimental data. The experimental values correspond to $T = 300$ K for α-U and ∼900 K for γ-U. MD calculations are performed at the same temperatures.

	EAM, this work	*Ab initio* [7]	*Ab initio* [8]	Experiment [49, 54]
		α-U		
a	2.8361	2.845	2.800	2.8537
b	5.7604	5.818	5.896	5.8695
c	4.9551	4.996	4.893	4.9548
y	0.1015	0.103	0.097	0.1025
V_0^{at}	20.238	20.674	20.194	20.747
E_{coh}	−4.20	—	—	−4.22 [55]
c_{11}	151	300	296	215
c_{22}	218	220	216	199
c_{33}	330	320	367	267
c_{12}	109	50	60	46
c_{13}	130	5	29	22
c_{23}	108	110	141	108
B	149	133	149	135.5
		γ-U		
a	3.493	—	3.430	3.470
V_0^{at}	21.309	—	20.180	20.890
B	95.0	—	176.0	113.3

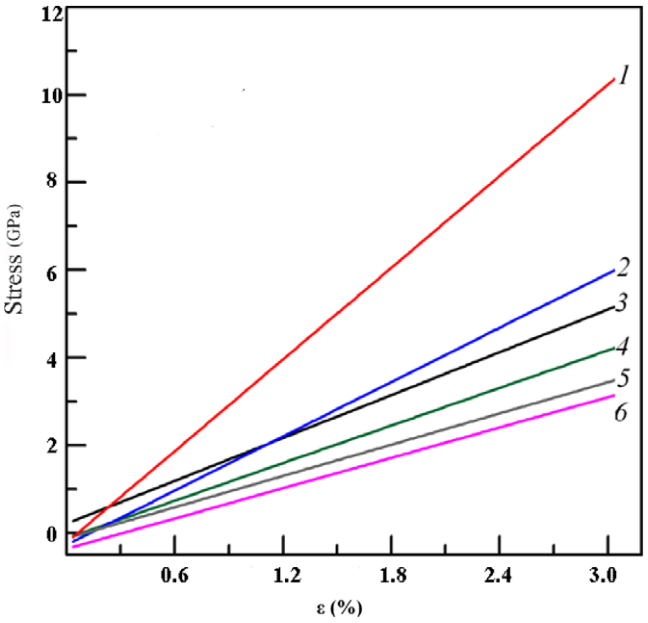

Figure 3. Changes of the components of stress tensor as a function of the compressing deformation ϵ (with the indication of the corresponding elastic constants): 1—changes in σ_{zz}, compression along the z-axis (gives c_{33}); 2—σ_{yy}, compression along the y-axis (c_{22}); 3—σ_{xx}, compression along the x-axis (c_{11}); 4—σ_{zz}, compression along the x-axis (c_{13}); 5—σ_{zz}, compression along the y-axis (c_{23}); 6—σ_{yy}, compression along the x-axis (c_{12}).

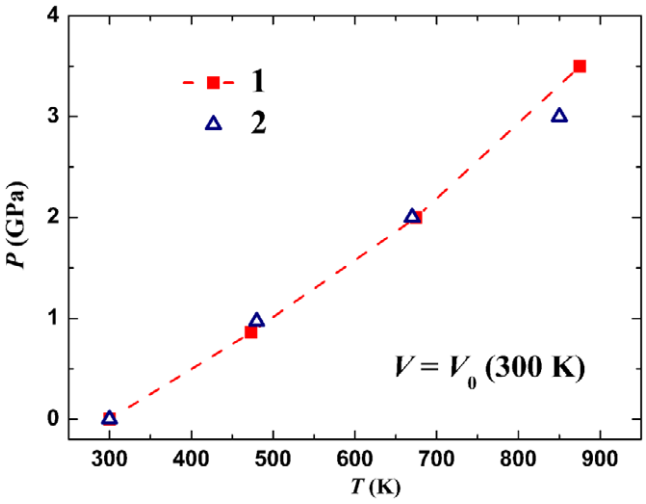

Figure 4. The normal density $V = V_0$ isochore of α-U: 1—experimental data [46]; 2—result of MD calculations with the potential obtained.

3.2. The normal density isochore of α-U

As another test we study the behaviour of the low-temperature orthorhombic α-U under isochoric heating. The obtained 'pressure–temperature' dependence compares well with the experimental data [46] (see figure 4). The mean thermal displacements of uranium atoms are not the same for different directions in α-U. The largest value is observed along the a-axis where the atoms are arranged closer to each other. This is consistent with the results of the diffraction study of anisotropy of thermal displacements in solid uranium [47].

3.3. The room-temperature isotherm of α-U

The uranium room-temperature isotherm is calculated in two different ways. First we carry out several independent calculations at the given V/V_0 ratios maintaining all stress

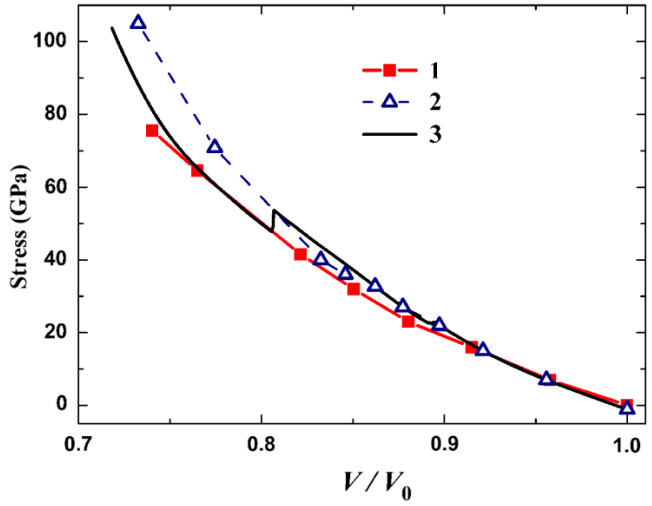

Figure 5. The room-temperature isotherms of α-U: 1—experimental data obtained with DAC [48, 49]; 2—results of MD calculations at $\sigma_{xx} = \sigma_{yy} = \sigma_{zz} = P$; 3—results obtained from the MD simulation of the uniform compression.

components equal to pressure P ($\sigma_{xx} = \sigma_{yy} = \sigma_{zz} = P$). While V/V_0 is no less then 0.8 the EAM isotherm is in good agreement with the diamond anvil cell (DAC) experiments, but during further compression the calculated curve becomes somewhat higher than the experimental one. As a second variant, a continuous uniform compression of the α-U is simulated. This approach does not allow us to keep all pressure components equal and the crystal structure deforms during the simulation. When $V/V_0 = 0.8$ the difference between σ_{xx} and σ_{zz} becomes larger than ~20 GPa and the deformation of the lattice becomes irreversible. It can be noticed from figure 5 that the 'pressure–volume' dependence obtained for this irreversibly deformed uranium during further compression is consistent with the experimental data [48, 49].

3.4. Bond-angle distribution functions for solid and liquid uranium

In order to understand how the potential reproduces the structure of solid and liquid U we calculate bond-angle distribution functions for several temperatures and compare them with the existing results of QMD simulations [11]. The bond-angle distribution function represents the number of bond angles that the given atom makes with its nearest neighbours. To define what atoms can be considered to be the nearest neighbours for the given atom we set the cut-off radius of 3.9 Å (equal to the value suggested in [11]). To perform the comparison we build two models of bcc U at low (330 K) and high (1680 K) temperatures as well as a model of liquid uranium at 2150 K. Each model has an atomic volume of 20.45 $Å^3$/atom. The resulting distributions are compared with the QMD data in figure 6. For each case one can see a good agreement between these two data sets. At 330 K the initial bcc U lattice becomes strongly distorted into a bct-like structure as was shown in [11] (γ-to-α transition is hindered due to the small system size).

Table 4. The energy of a single vacancy formation in α-U (eV).

EAM MD [31]	*ab initio* [8]	*ab initio* [12]	EAM, this work
1.50	1.95	1.86	2.14

Table 5. The energy of a single vacancy formation in γ-U (eV).

EAM MD [31]	*ab initio* [10]	*ab initio* [12]	Expt. [56]	EAM, this work
1.75	1.08	1.384	1.20 ± 0.25	1.52

3.5. Energy of a single vacancy formation

A proper description of defect formation in the solid state is crucial for radiation damage studies. That is why a single vacancy formation energy is an important basic test of the new potential. This energy is determined as follows:

$$E^{\mathrm{f}}_{\mathrm{vac}} = E_{N-1} - \frac{N-1}{N} E_N. \qquad (6)$$

Here N is the number of atoms in the model of the ideal crystal lattice without vacancies. E_N is the energy of this ideal lattice and E_{N-1} corresponds to the model that contains a single vacancy. We perform structural relaxations for the models of perfect single crystal uranium with and without a single vacancy for determination of the corresponding energy values. The α-U model contains 5200 atoms in the simulation box with 3D PBC. For γ-U we use 250 atoms and the structural relaxation is performed only for a part of the system in order to overcome spontaneous bcc lattice distortion at low temperatures [12]. The results obtained for both solid structures of uranium are presented in tables tables 4 and 5. For α-U the experimental value of the vacancy formation energy is known while for γ-U it was only estimated by the DFT method.

4. Melting and α–γ transition

We calculate the melting line and the temperature of the α–γ transition at the given pressure. In both cases we use the two-phase simulation technique (e.g. see [50–53]). Fragments of the simulation boxes are presented in figure 7.

The simulations are performed in 3D PBC. One part of the box is filled by the bcc lattice of uranium atoms and another part is filled with liquid uranium. The total number of atoms is 20 250. The algorithm of the calculation includes equilibration of the system at the given pressure for ~50 ps. Depending on the temperature and pressure the phase boundary can move or remain stable. In the latter case both phases coexist in equilibrium, which gives the value of the melting temperature at the given pressure.

The structure of the simulation box used for the calculation of the solid–solid α–γ transition is shown in figure 7(b). The algorithm of the calculation remains the same as described above for melting. The model contains 16 800

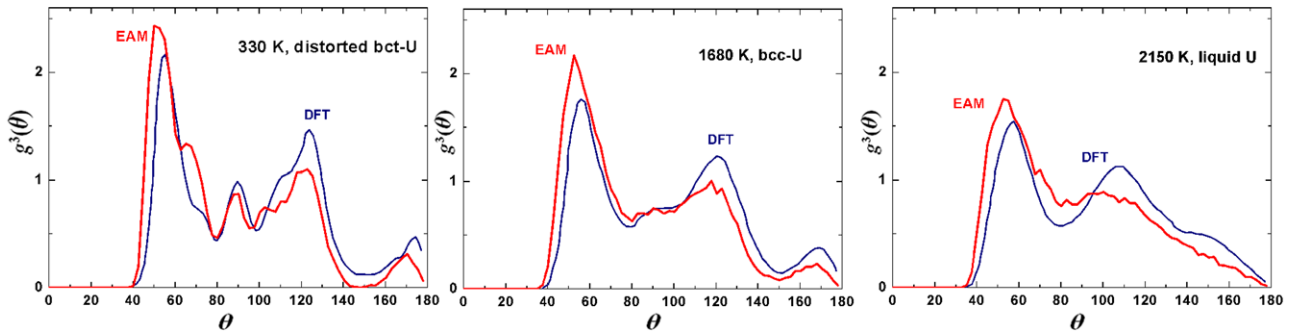

Figure 6. Bond-angle distribution functions $g^3(\theta)$ calculated with the EAM potential developed in the present work in comparison with the QMD results [11]. At 330 K the initial bcc γ-U lattice is strongly distorted into a bct-like structure.

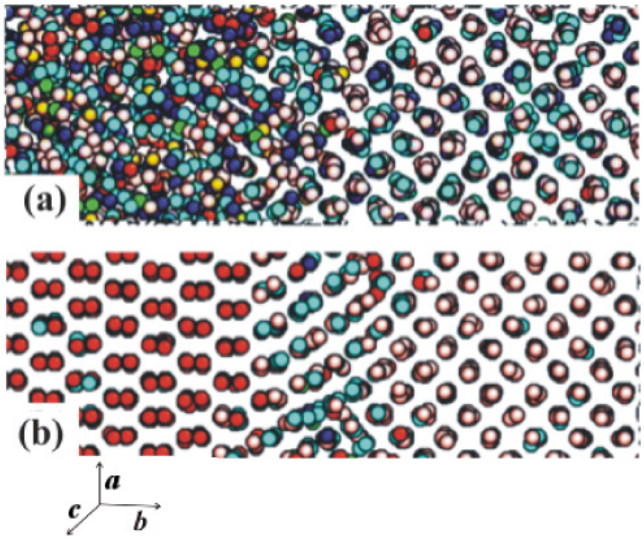

Figure 7. Fragments of the two-phase simulation boxes: the phase boundary between liquid and bcc γ-U solid (a) and the boundary between α-U and γ-U (b). γ-U is on the right. Projections of all atoms in the simulation box on a plane are presented in both pictures; arrows show the orientation of the α-U lattice.

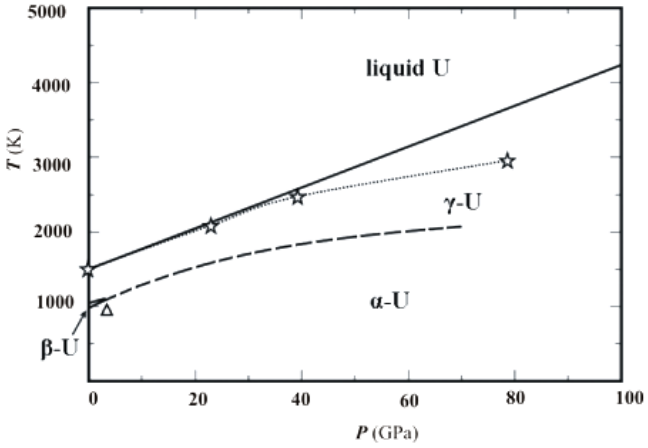

Figure 8. The P–T phase diagram of uranium. The experimental results [49] are shown by the solid line (the melting curve) and the dashed line (the α–γ transition curve); the melting curve calculated with the EAM potential is shown by the stars; the calculated temperature of the α–γ transition at 3 GPa is marked by a triangle.

atoms in 3D PBC. The time length of the MD simulation is about 10 ns. To exclude the possible effects of the β-U we study a compressed system at 3 GPa. When the temperature is lower than 800 K the growth of the low-temperature α-U is observed. At $T > 800$ K α-U transforms to γ-U. At 800 K these two allotropes coexist in equilibrium. Therefore we can estimate that the temperature of the α–γ transition at 3 GPa is about 800 ± 50 K, which agrees well with the experimental value.

All the calculated results are presented in figure 8 in comparison with the results of the *in situ* DAC x-ray/laser-heating experiments [49].

5. Conclusion

Using the force-matching method we developed a new interatomic EAM potential for uranium aimed at simulation of α-U, γ-U and liquid uranium, the corresponding transitions between them as well as the radiation damage. The results of the performed MD test calculations confirm that it is possible to obtain a good quantitative description of the structure and properties of the solid uranium allotropes using a relatively simple EAM model. The lattice constants, bulk modulus, bond-angle distribution functions, the room-temperature isotherm, normal density isochore and the single vacancy formation energy for α and γ structures computed using this potential agree well with the reported experimental and *ab initio* data. The calculated melting line of uranium at pressures up to 80 GPa and the temperature of the solid–solid α–γ transition at 3 GPa are both in good agreement with the experimental data. Hence this new EAM uranium potential provides an overall quantitative description of the properties of liquid and solid uranium at pressures from 0 to 80 GPa and temperatures up to 2500 K.

Acknowledgments

The calculations were carried out on the computing clusters MIPT-60 of the Moscow Institute of Physics and Technology, MVS-100K of the Joint Supercomputer Center of RAS and 'Lomonosov' of the Moscow State University. The work was

supported by the Program for Basic Research of the RAS No. 2, the RFBR 09-08-01116 grant and the President RF grant MK-3174.2011.8 (VVS).

References

[1] Hofman G L, Walters L C and Bauer T H 1997 *Prog. Nucl. Energy* **31** 83–110
[2] Meyer M K, Hofman G L, Hayes S L, Clark C R, Wiencek T C, Snelgrove J L, Strain R V and Kim K-H 2002 *J. Nucl. Mater.* **304** 221–36
[3] Kim Y S, Hofman G and Yacout A 2009 *J. Nucl. Mater.* **392** 164–70
[4] Carmack W J, Porter D L, Chang Y I, Hayes S L, Meyer M K, Burkes D E, Lee C B, Mizuno T, Delage F and Somers J 2009 *J. Nucl. Mater.* **392** 139–50
[5] Wirth B D 2007 *Science* **318** 923–4
[6] Bai X M, Voter A F, Hoagland R G, Nastasi M and Uberuaga B P 2010 *Science* **327** 1631–4
[7] Söderlind P 2002 *Phys. Rev.* B **66** 085113
[8] Taylor C 2008 *Phys. Rev.* B **77** 1–9
[9] Kresse G 1999 *Phys. Rev.* B **59** 1758–75
[10] Xiang S, Huang H and Hsiung L 2008 *J. Nucl. Mater.* **375** 113–9
[11] Hood R, Yang L and Moriarty J 2008 *Phys. Rev.* B **78** 094119
[12] Beeler B, Good B, Rashkeev S, Deo C, Baskes M and Okuniewski M 2010 *J. Phys.: Condens. Matter* **22** 505703
[13] Huang G Y and Wirth B D 2011 *J. Phys.: Condens. Matter* **23** 205402
[14] Landa A, Söderlind P and Turchi P 2011 *J. Nucl. Mater.* **414** 132–7
[15] Ackland G J and Thetford R 1987 *Phil. Mag.* A **56** 15–30
[16] Chernov V M, Romanov V A and Krutskikh A O 1999 *J. Nucl. Mater.* **271/272** 274–9
[17] Belonoshko A, Ahuja R, Eriksson O and Johansson B 2000 *Phys. Rev.* B **61** 3838–44
[18] Mishin Y, Mehl M, Papaconstantopoulos D, Voter A and Kress J 2001 *Phys. Rev.* B **63** 1–16
[19] Li Y, Siegel D, Adams J and Liu X Y 2003 *Phys. Rev.* B **67** 125101
[20] Mendelev M I, Han S, Srolovitz D J, Ackland G J, Sun D Y and Asta M 2003 *Phil. Mag.* **83** 3977–94
[21] Olsson P, Wallenius J, Domain C, Nordlund K and Malerba L 2005 *Phys. Rev.* B **72** 214119
[22] Dudarev S L and Derlet P M 2005 *J. Phys.: Condens. Matter* **17** 7097–118
[23] Mendelev M I and Ackland G J 2007 *Phil. Mag. Lett.* **87** 349–59
[24] Mendelev M, Han S, Son W J, Ackland G and Srolovitz D 2007 *Phys. Rev.* B **76** 1098–0121
[25] Hennig R, Lenosky T, Trinkle D, Rudin S and Wilkins J 2008 *Phys. Rev.* B **78** 1–10
[26] Stoller R, Golubov S, Kamenski P, Seletskaia T and Osetsky Y 2010 *Phil. Mag.* **90** 923–34
[27] Derlet P, Gilbert M and Dudarev S 2011 *Phys. Rev.* B **84** 19–21
[28] Starikov S, Insepov Z, Rest J, Kuksin A Y, Norman G, Stegailov V and Yanilkin A 2011 *Phys. Rev.* B **84** 104109
[29] Insepov Z, Rest J, Yacout A, Kuksin A, Norman G, Stegailov V, Starikov S and Yanilkin A 2011 *J. Nucl. Mater.* in press
[30] Pascuet M I, Fernández J R and Monti A M 2007 *Anal. AFA* **19** 40–5
[31] Pascuet M I, Fernández J R and Monti A M 2008 *Proc. Int. Conf. 'Multiscale Modeling of Microstructure Evolution in Materials'* p 489
[32] Belashchenko D K, Smirnova D E and Ostrovski O I 2010 *High Temp.* **48** 363–75
[33] Li R, He B and Zhang Q 2011 *Chin. J. Chem. Phys.* **24** 405–11
[34] Daw M and Baskes M 1983 *Phys. Rev. Lett.* **50** 1285–8
[35] Daw M and Baskes M 1984 *Phys. Rev.* B **29** 6443–53
[36] Finnis M W and Sinclair J E 1984 *Phil. Mag.* A **50** 45–55
[37] Ercolessi F, Tosatti E and Parrinello M 1986 *Phys. Rev. Lett.* **57** 719–22
[38] Ercolessi F, Parrinello M and Tosatti E 1988 *Phil. Mag.* A **58** 213–26
[39] Ercolessi F and Adams J B 1994 *Europhys. Lett.* **26** 583–8
[40] Fellinger M, Park H and Wilkins J 2010 *Phys. Rev.* B **81** 144119
[41] Plimpton S 1995 *J. Comput. Phys.* **117** 1–19
[42] Kresse G 1996 *Phys. Rev.* B **54** 11169–86
[43] Perdew J P and Wang Y 1992 *Phys. Rev.* B **45** 13244–9
[44] Brommer P and Gähler F 2006 *Phil. Mag.* **86** 753–8
[45] Brommer P and Gähler F 2007 *Modell. Simul. Mater. Sci. Eng.* **15** 295–304
[46] Zhao Y, Zhang J, Brown D, Korzekwa D, Hixson R and Wang L 2007 *Phys. Rev.* B **75** 174104
[47] Blanter M S, Glazkov V P and Somenkov V A 2009 *Phys. Status Solidi* b **246** 1044–9
[48] Akella J, Smith G S, Grover R, Wu Y and Martin S 1990 *High Pressure Res.* **2** 295–302
[49] Yoo C S, Cynn H and Söderlind P 1998 *Phys. Rev.* B **57** 10359–62
[50] Morris J, Wang C, Ho K and Chan C 1994 *Phys. Rev.* B **49** 3109–15
[51] Belonoshko A 1994 *Geochim. Cosmochim. Acta* **58** 4039–47
[52] Koči L, Ahuja R and Belonoshko A 2007 *Phys. Rev.* B **75** 214108
[53] Starikov S V and Stegailov V V 2009 *Phys. Rev.* B **80** 220104(R)
[54] Barrett C, Mueller M and Hitterman R 1963 *Phys. Rev.* **129** 625–9
[55] Kaptay G, Csicsovszki G and Yaghmaee M S 2003 *Mater. Sci Forum* **414/415** 235–40
[56] Matter H, Winter J and Triftshauser W 1980 *J. Nucl. Mater.* **88** 273–8